

Supporting Information

Metabolic profiling of neocortical tissue discriminates Alzheimer's disease from mild cognitive impairment, high pathology controls, and normal controls

Paniz Jasbi¹⁺, Xiaojian Shi^{1,2+}, Ping Chu³, Natalie Elliott³, Haley Hudson³, Douglas Jones⁴, Geidy Serrano⁵, Brandon Chow¹, Thomas G. Beach⁵, Li Liu^{6,7}, Garilyn Jentarra^{3,8*}, Haiwei Gu^{1*}

¹Arizona Metabolomics Laboratory, College of Health Solutions, Arizona State University, Phoenix, AZ 85004, USA

²Systems Biology Institute, Cellular and Molecular Physiology, Yale School of Medicine, West Haven, CT 06516, USA

³Department of Biochemistry and Molecular Genetics, ⁴Department of Pharmacology, Midwestern University, Glendale, AZ 85308, USA

⁵Banner Sun Health Research Institute, Sun City, AZ 85351, USA

⁶College of Health Solutions, Biodesign Institute, Arizona State University, Tempe, Arizona 85281, USA

⁷Department of Neurology, Mayo Clinic, Scottsdale, Arizona 85259, USA

⁸Precision Medicine Program, Midwestern University, Glendale, AZ 85308, USA

⁺Authors contributed equally

^{*}Corresponding authors

Page S-4: Table S1. Matrix of correlation analysis between candidate markers and clinical characteristics showing r and (p).

Page S-6: Table S2. Full list of significantly enriched enzymes in response to Alzheimer's progression. For analysis, subjects were dichotomously grouped as case (MCI and AD) and control (NC and HPC).

Page S-7: Figure S1. Scores plot of principal component analysis (PCA) conducted with all reliably detected metabolites between all groups, including quality control (QC) samples; 95% confidence intervals were evaluated for potential outliers. Data for sample 13 (HPC group) was reviewed and removed from further analysis.

Page S-8: Figure S2. Significant metabolites between case (AD and MCI) and control (HPC and NC) as determined by independent samples t-test. Data were \log_{10} -transformed and Pareto scaled prior to plotting.

Page S-9: Figure S3. ROC analysis of PLS-DA model constructed using levels of lauric acid, myristic acid, stearic acid, and palmitic acid (all $p < 0.05$): (A) classification of NC vs. HPC/MCI/AD, (B) classification of HPC vs. NC/MCI/AD, (C) classification of MCI vs. NC/HPC/AD, and (D) classification of AD vs. NC/HPC/MCI.

Page S-10: Figure S4. (A) RF analysis of study groups based on levels of lauric acid, myristic acid, stearic acid, palmitic acid (OOB error = 0.511), and (B) 100-fold LOOCV ROC analysis of case (MCI/AD) and control (NC/HPC) using RF classifier (AUC = 0.917).

Page S-11: Figure S5. Univariate ROC analysis and t-testing between NC and MCI groups show lauric acid to be highly predictive (AUC = 0.993) and significant (FDR $q < 0.001$).

Page S-12: Figure S6. Univariate ROC analysis and t-testing between NC and AD groups show lauric acid to be highly predictive (AUC = 1.0) and significant (FDR $q < 0.001$).

Page S-13: Figure S7. Univariate ROC analysis and t-testing of between HPC and AD groups show high predictive performance (AUC > 0.90) and significance (FDR $q < 0.01$) of myristic acid, lauric acid, palmitic acid, and stearic acid.

Page S-14: Figure S8. (A) Scores plot of PLS-DA model constructed using significant between-group metabolites (lauric acid, myristic acid, stearic acid, palmitic acid) in conjunction with highly correlated neuropathological characteristics (frontal plaque, total plaque, total tangle, and Braak score) ($R^2X = 0.710$, $R^2Y = 0.748$, $R^2Q = 0.722$) and (B) Permutation testing with 100 iterations shows excellent model fit ($p < 0.01$).

Page S-15: Figure S9. Network view of enzyme enrichment analysis conducted between case (MCI and AD) and control (NC and HPC). Enrichment ratios were significantly different for eleven enzymes between groups ($p < 0.05$).

Table S1. Matrix of correlation analysis between candidate markers and clinical characteristics showing *r* and (*p*).

Clinical Characteristic	272.2@20.932005	147.1@14.3080015	147.1@20.774895	73.1@27.868113	Lauric acid	Myristic acid	Palmitoleic acid	Palmitic acid	Stearic acid
Age	-0.079 (0.598)	0.048 (0.748)	-0.036 (0.810)	-0.103 (0.490)	-0.043 (0.775)	0.150 (0.313)	0.210 (0.157)	0.168 (0.259)	0.168 (0.259)
Sex	0.116 (0.437)	-0.246 (0.095)	-0.012 (0.936)	-0.100 (0.505)	-0.071 (0.638)	0.104 (0.488)	0.234 (0.114)	0.181 (0.222)	0.136 (0.360)
PMI	0.219 (0.139)	0.019 (0.897)	0.183 (0.217)	-0.078 (0.604)	-0.269 (0.067)	-0.221 (0.135)	-0.222 (0.134)	-0.149 (0.318)	-0.154 (0.302)
APOE alleles	-0.045 (0.762)	0.048 (0.751)	-0.047 (0.755)	-0.084 (0.574)	0.092 (0.538)	0.051 (0.733)	0.058 (0.699)	0.031 (0.839)	0.043 (0.777)
MMSE	-0.097 (0.515)	0.114 (0.445)	-0.064 (0.669)	0.362 (0.012)	0.363 (0.012)	0.398 (0.006)	0.202 (0.172)	0.278 (0.059)	0.294 (0.045)
Frontal plaque	0.198 (0.182)	-0.036 (0.810)	0.130 (0.382)	-0.160 (0.283)	-0.598 (0.000)	-0.085 (0.569)	0.118 (0.428)	0.003 (0.982)	-0.004 (0.981)
Total Plaque	0.296 (0.043)	-0.092 (0.539)	0.157 (0.293)	-0.153 (0.305)	-0.579 (0.000)	-0.100 (0.503)	0.108 (0.469)	-0.001 (0.993)	-0.002 (0.988)
Frontal Tangle	0.203 (0.172)	-0.129 (0.387)	0.070 (0.639)	-0.141 (0.345)	-0.410 (0.004)	-0.399 (0.005)	-0.109 (0.467)	-0.289 (0.048)	-0.276 (0.061)
Total Tangle	0.111 (0.457)	-0.200 (0.177)	0.148 (0.322)	-0.246 (0.096)	-0.507 (0.000)	-0.350 (0.016)	-0.011 (0.941)	-0.219 (0.138)	-0.229 (0.122)

Braak score	0.063 (0.672)	-0.157 (0.293)	0.198 (0.182)	-0.252 (0.087)	-0.539 (0.000)	-0.353 (0.015)	-0.046 (0.757)	-0.234 (0.113)	-0.250 (0.091)
Frontal CAA	0.105 (0.481)	0.036 (0.811)	0.179 (0.228)	-0.165 (0.267)	-0.169 (0.257)	0.094 (0.529)	0.274 (0.063)	0.209 (0.159)	0.196 (0.187)
Total CAA	0.100 (0.502)	0.005 (0.972)	0.083 (0.579)	-0.164 (0.269)	-0.211 (0.155)	0.091 (0.543)	0.295 (0.044)	0.219 (0.139)	0.194 (0.191)

Table S2. Full list of significantly enriched enzymes in response to Alzheimer's progression. For analysis, subjects were dichotomously grouped as case (MCI and AD) and control (NC and HPC).

Enzyme	<i>p</i> value
Mitochondrial 2-oxovalerate dehydrogenase	0.025
3-amino-isobutyrate transport	0.025
Mitochondrial 3-amino-isobutyrate transport	0.025
3-hydroxyacyl-CoA dehydratase	0.025
Mitochondrial 3-hydroxyisobutyrate dehydrogenase	0.025
Mitochondrial 3-hydroxyisobutyryl-CoA hydrolase	0.025
Mitochondrial acyl-CoA dehydrogenase	0.025
L-3-amino-isobutanoate exchange	0.025
Mitochondrial L-3-aminoisobutyrate transaminase	0.025
Mitochondrial malonate-semialdehyde dehydrogenase	0.025
Methylmalonate-semialdehyde dehydrogenase	0.025

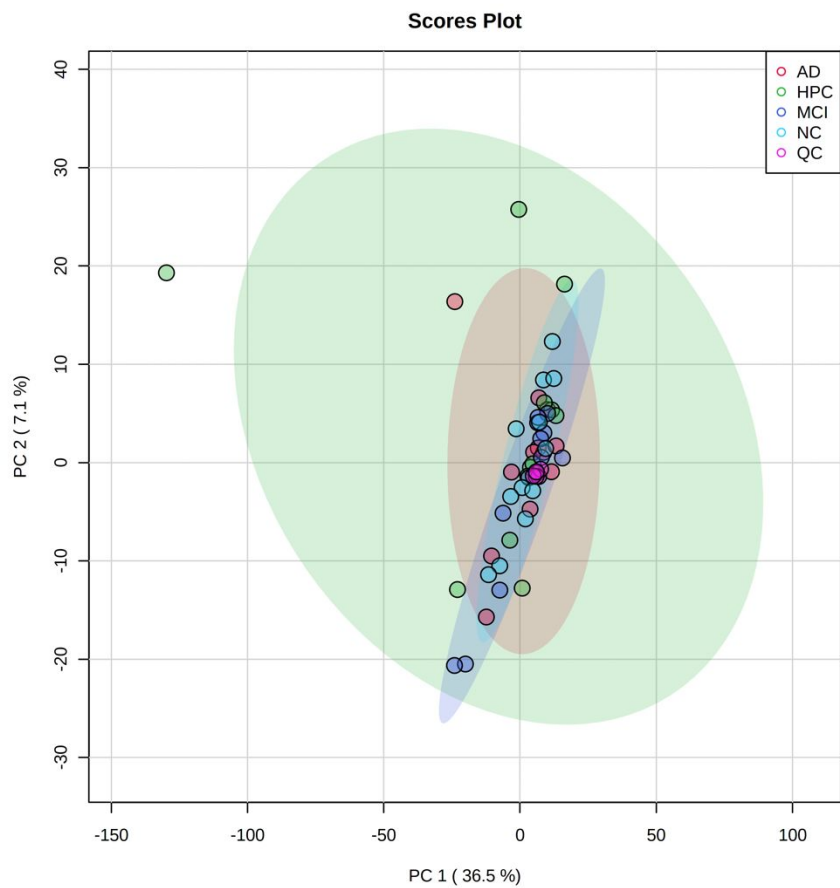


Figure S1. Scores plot of principal component analysis (PCA) conducted with all reliably detected metabolites between all groups, including quality control (QC) samples; 95% confidence intervals were evaluated for potential outliers. Data for sample 13 (HPC group) was reviewed and removed from further analysis.

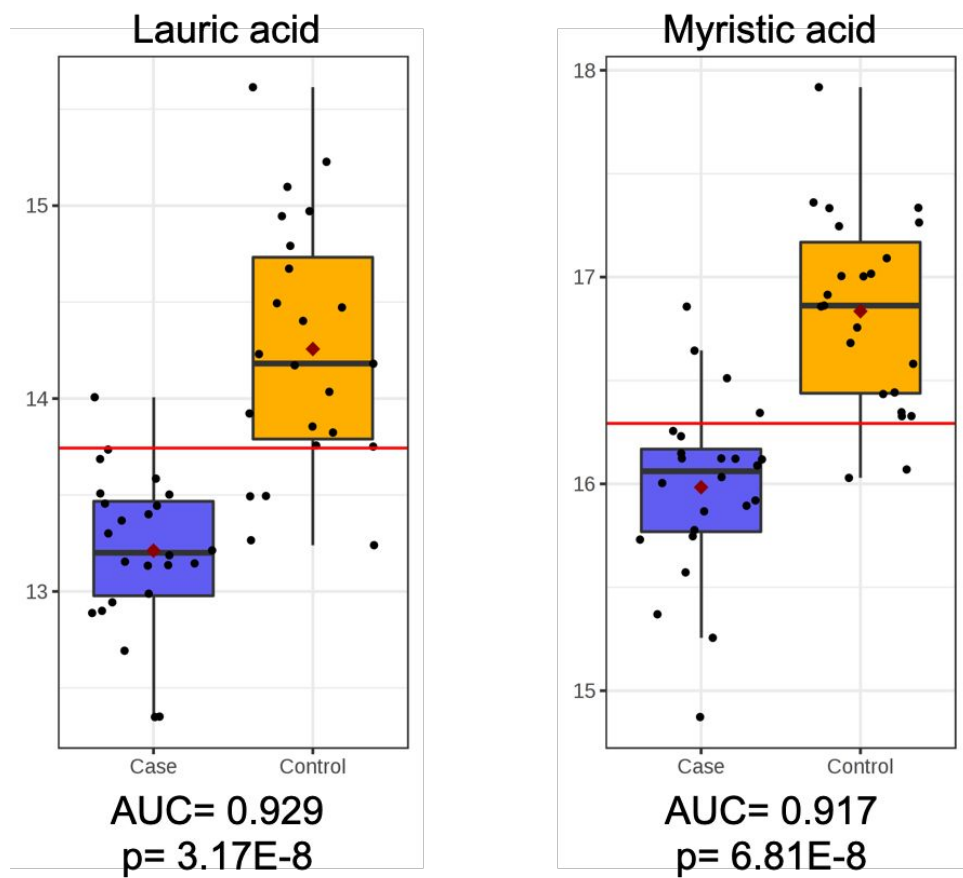


Figure S2. Significant metabolites between case (MCI and AD) and control (NC and HPC) as determined by independent samples t-test. Data were log₁₀-transformed and Pareto scaled prior to plotting.

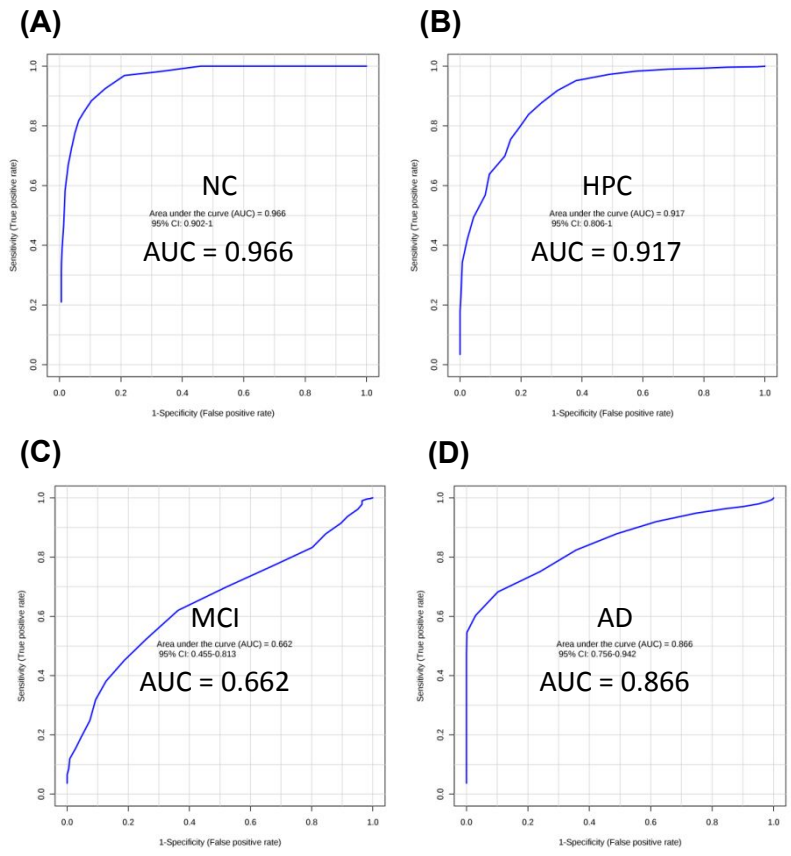


Figure S3. ROC analysis of PLS-DA model constructed using levels of lauric acid, myristic acid, stearic acid, and palmitic acid (all $p < 0.05$): (A) classification of NC vs. HPC/MCI/AD, (B) classification of HPC vs. NC/MCI/AD, (C) classification of MCI vs. NC/HPC/AD, and (D) classification of AD vs. NC/HPC/MCI.

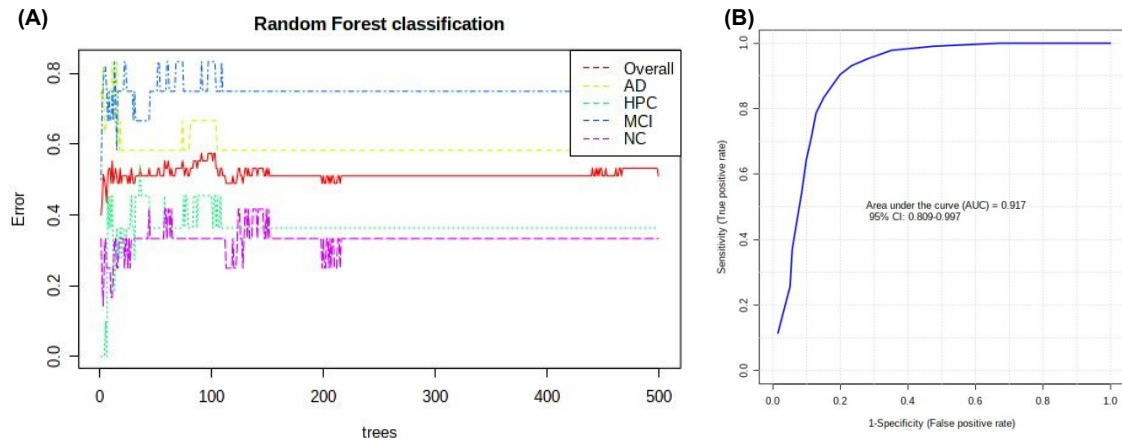


Figure S4. (A) RF analysis of study groups based on levels of lauric acid, myristic acid, stearic acid, palmitic acid (OOB error = 0.511), and (B) 100-fold LOOCV ROC analysis of case (MCI/AD) and control (NC/HPC) using RF classifier (AUC = 0.917).

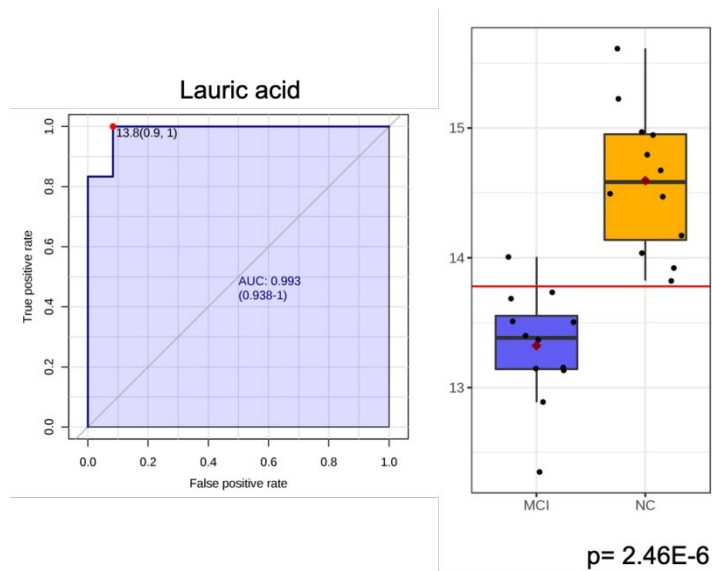


Figure S5. Univariate ROC analysis and t-testing between NC and MCI groups show lauric acid to be highly predictive (AUC = 0.993) and significant (FDR $q < 0.001$).

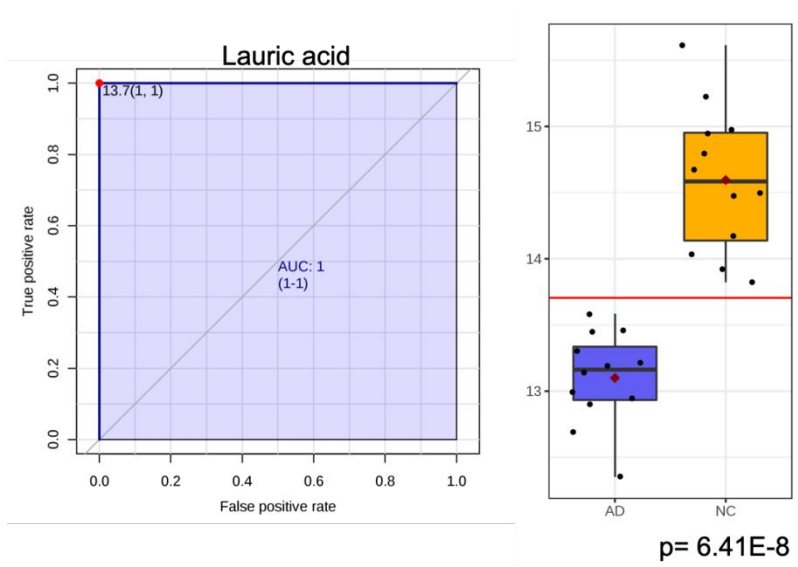


Figure S6. Univariate ROC analysis and t-testing between NC and AD groups show lauric acid to be highly predictive (AUC = 1.0) and significant (FDR $q < 0.001$).

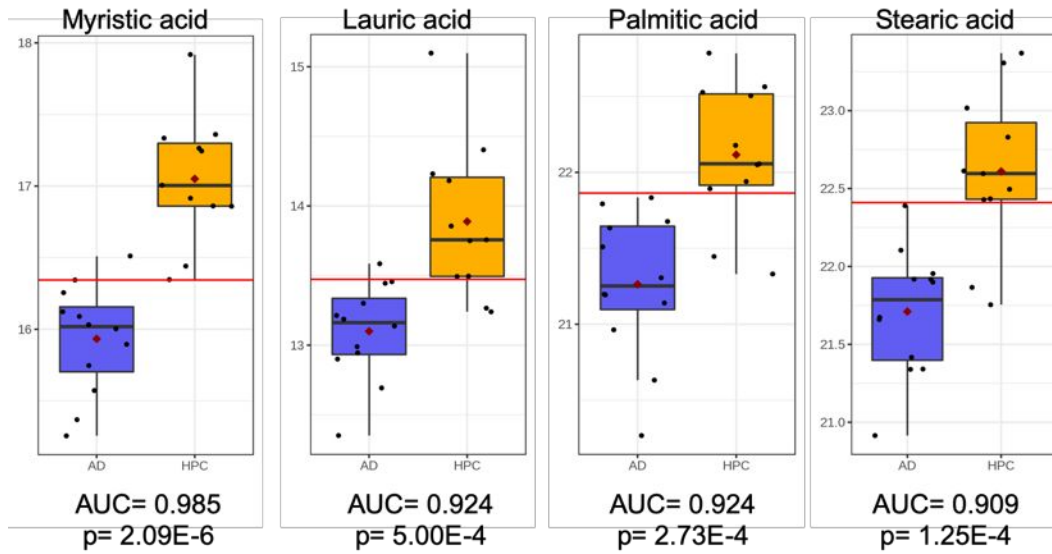


Figure S7. Univariate ROC analysis and t-testing of between HPC and AD groups show high predictive performance ($AUC > 0.90$) and significance ($FDR q < 0.01$) of myristic acid, lauric acid, palmitic acid, and stearic acid.

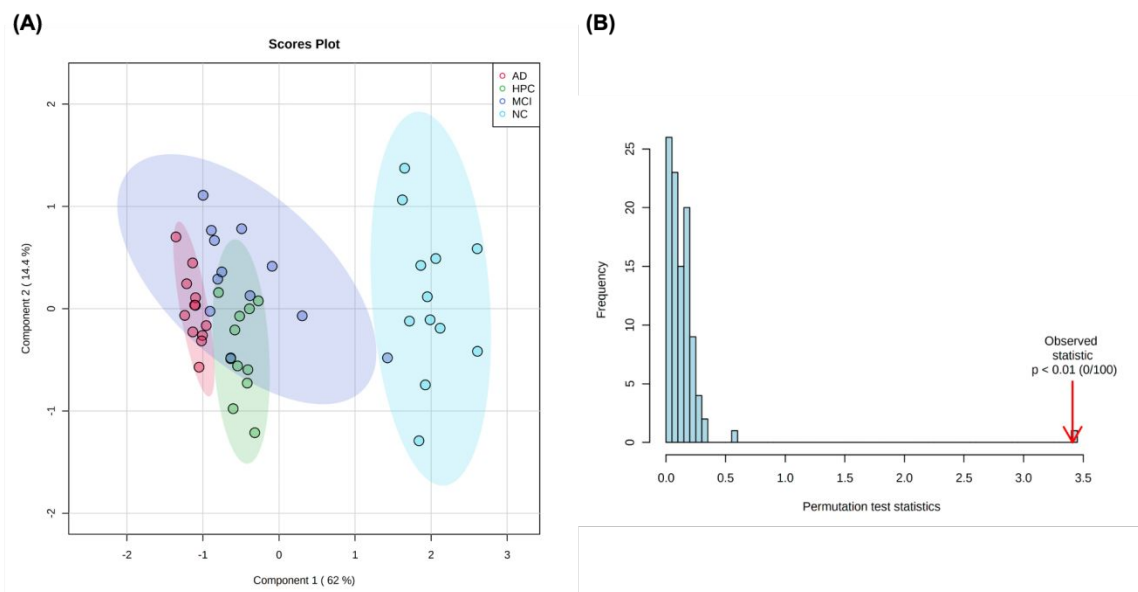


Figure S8. (A) Scores plot of PLS-DA model constructed using significant between-group metabolites (lauric acid, myristic acid, stearic acid, palmitic acid) in conjunction with highly correlated neuropathological characteristics (frontal plaque, total plaque, total tangle, and Braak score) ($R^2X = 0.710$, $R^2Y = 0.748$, $R^2Q = 0.722$) and (B) Permutation testing with 100 iterations shows excellent model fit ($p < 0.01$).

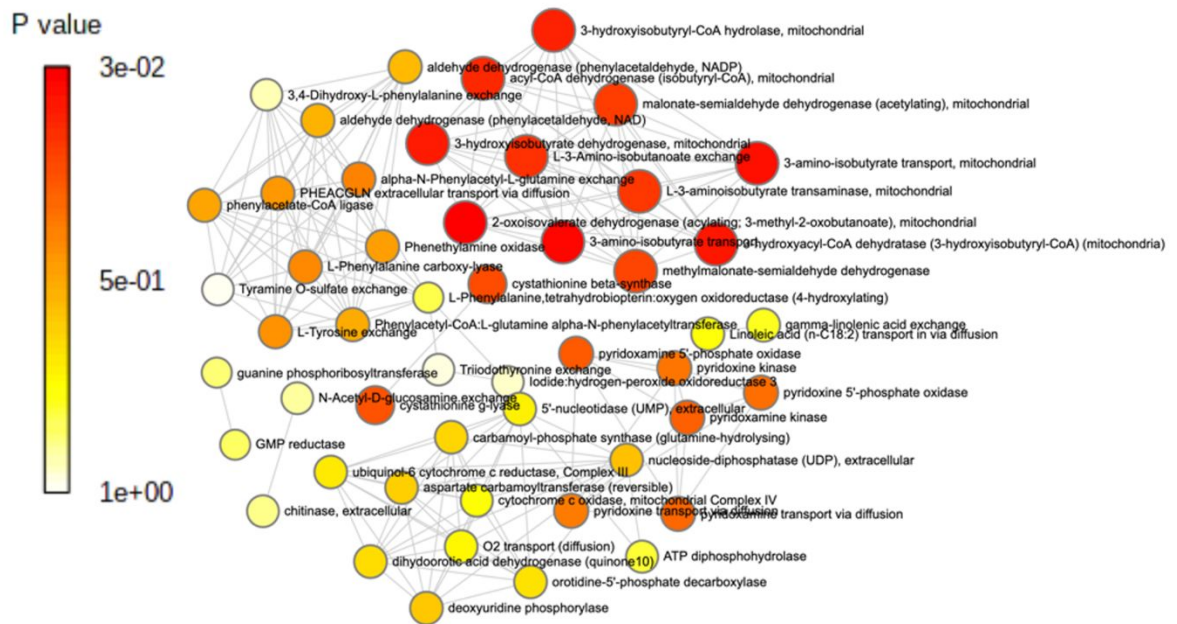


Figure S9. Network view of enzyme enrichment analysis conducted between case (MCI and AD) and control (NC and HPC). Enrichment ratios were significantly different for eleven enzymes between groups ($p < 0.05$).